

# The stationary density matrix of a pumped polariton system

Carlos Andrés Vera<sup>(a)</sup>, Alejandro Cabo<sup>(b)</sup>, and Augusto González<sup>(b)</sup>  
<sup>(a)</sup>*Instituto de Física, Universidad de Antioquia, AA 1226, Medellín, Colombia*

<sup>(b)</sup>*Instituto de Cibernética, Matemática y Física, Calle E 309, Vedado, Ciudad Habana, Cuba*

The density matrix,  $\rho$ , of a model polariton system is obtained numerically from a master equation which takes account of pumping and losses. In the stationary limit, the coherences between eigenstates of the Hamiltonian are three orders of magnitude smaller than the occupations, meaning that the stationary density matrix is approximately diagonal in the energy representation. A weakly distorted grand canonical Gibbs distribution fits well the occupations.

PACS numbers: 71.36.+c,42.50.Ct,05.70.Ln

The possibility of Bose-Einstein condensation (BEC) of excitonic polaritons in microcavities has raised big expectations recently [1, 2, 3]. Due to the relatively small lifetimes of polaritons (of the order of picoseconds) and still smaller rates for phonon relaxation in the lower polariton branch [4], a very important question should be answered concerning whether the observed magnitudes come from a system in thermal equilibrium or have a dynamical nature.

In paper [5], we show that in a decaying system the enhancement of ground-state occupations can be understood in terms of the combined effects of polariton-polariton scattering and photon emission, even if phonon relaxation does not act. This suggests that the results of the experiment reported in [1] could be ascribed to a dynamical effect and not necessarily to BEC in the polariton system.

On the other hand, in the continuously pumped system, where a stationary state is reached when pump and losses are equilibrated, it was undoubtedly demonstrated that phonon relaxation is not effective in the lower polariton states [6]. Thus, the question arises about what kind of stationary state are we reaching in the experiments reported in [2].

In the present paper, we are aimed at giving a partial answer to the latter question. We will assume that there are not thermalization mechanisms, and will compute the density matrix arising from a purely dynamical equation. We use the same model of polariton system, previously studied in Refs. [5, 7], with a finite number of single-particle states for electrons and holes and a single photon mode in the microcavity. A term accounting for pumping is added to the master equation for the density matrix. This master equation is numerically solved in order to find the stationary density matrix. The main result of the paper is the following: in the stationary limit the density matrix is approximately diagonal in the energy representation and, thus, describes a kind of quasiequilibrium which can be fitted to a weakly distorted grand canonical Gibbs distribution. The distorted Gibbs distribution can be thought of as coming from the maximization of the entropy with an additional

constraint in phase space commuting with the Hamiltonian and fulfilling the requirement of additivity. This idea was presented in Ref. [8] to describe quasi-stationary nonequilibrium states and share similarities with the results of Hamiltonian dynamics simulations [9].

For completeness, we first recall the main features of the model polariton system. The Hamiltonian describing the system is the following:

$$\begin{aligned}
 H = & \sum_i \left\{ T_i^{(e)} e_i^\dagger e_i + T_i^{(h)} h_i^\dagger h_i \right\} \\
 & + \frac{\beta}{2} \sum_{ijkl} \langle ij || kl \rangle e_i^\dagger e_j^\dagger e_l e_k + \frac{\beta}{2} \sum_{\bar{i}\bar{j}\bar{k}\bar{l}} \langle \bar{i}\bar{j} || \bar{k}\bar{l} \rangle h_i^\dagger h_j^\dagger h_{\bar{l}} h_{\bar{k}} \\
 & - \beta \sum_{\bar{i}\bar{j}\bar{k}\bar{l}} \langle \bar{i}\bar{j} || \bar{k}\bar{l} \rangle e_i^\dagger h_j^\dagger h_{\bar{l}} e_k + (E_{gap} + \Delta) a^\dagger a \\
 & + g \sum_i \left\{ a^\dagger h_i e_i + a e_i^\dagger h_i \right\}. \tag{1}
 \end{aligned}$$

We include 10 single-electron and 10 single-hole levels in Eq. (1) (the first three two-dimensional harmonic oscillator shells). The single-particle spectrum for electrons and holes is assumed flat:

$$T_i^{(e)} = E_{gap}, \quad T_i^{(h)} = 0. \tag{2}$$

This means that the dot confinement energy,  $\hbar\omega_0$ , is assumed much smaller than the effective band gap,  $E_{gap}$ . Our model describes a relatively small quantum dot strongly interacting with the lowest photon mode of a thin microcavity.  $\beta$  is the characteristic Coulomb energy,  $\beta = e^2/(4\pi\epsilon l_{osc}) = e^2/(4\pi\epsilon)\sqrt{m\omega_0}/\hbar$ , where  $\epsilon$  is the medium dielectric constant, and  $l_{osc} = \sqrt{\hbar/(m\omega_0)}$  – the oscillator length. We will take the value,  $\beta = 2$  meV.  $\langle ij || kl \rangle$  are matrix elements of the Coulomb interaction between harmonic oscillator states. The parameter  $\Delta$  gives the detuning of the photon energy with respect to the (bare) pair energy, equal to  $E_{gap}$ , and  $g = 3$  meV is the photon-matter coupling strength. Notice that the photon couples the electron state  $i$  to the hole state  $\bar{i}$ , which differs from the latter only in the sign of the angular momentum. This means that electron-hole pairs are

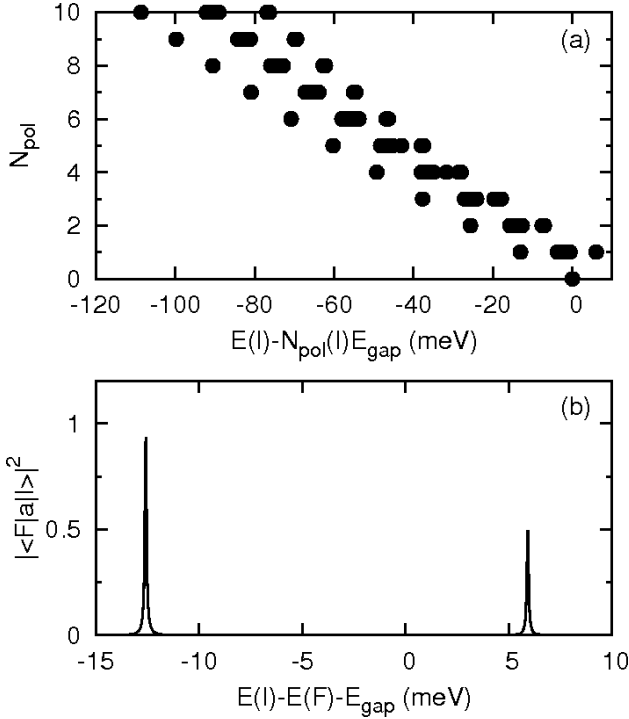


FIG. 1: (a) The lowest states in sectors with  $0 \leq N_{pol} \leq 10$ . (b) The matrix elements  $|\langle F|a|I\rangle|^2$ , smeared with a Lorentzian of width  $\Gamma = 0.1$  meV, vs the energy difference  $E(I) - E(F) - E_{gap}$ . The states  $|I\rangle$  correspond to  $N_{pol} = 2$ , whereas  $|F\rangle$  is the ground state in the  $N_{pol} = 1$  sector

created or annihilated in states with zero angular momentum. As a result, the Hamiltonian, Eq. (1), commutes with the total angular momentum of the system,  $L_{total}$ . In what follows, we consider only  $L_{total} = 0$  states.

The Hamiltonian, Eq. (1), preserves the polariton number,

$$N_{pol} = a^\dagger a + \sum_i (\hbar_i^\dagger \hbar_i + e_i^\dagger e_i) / 2. \quad (3)$$

We diagonalize the Hamiltonian in a basis constructed from Slater determinants for electrons and holes and Fock states of photons. For a given polariton number,  $N_{pol}$ , the wave functions are looked for as linear combinations:

$$|I\rangle = \sum C_{S_e, S_h, n} |S_e, S_h, n\rangle. \quad (4)$$

where  $S_e$  and  $S_h$  are Slater determinants with the same number of particles,  $N_{pairs}$ , and  $n = N_{pol} - N_{pairs}$ . When  $N_{pol} = 0$  there is only one state, the vacuum. When  $N_{pol} = 1$  there are 17 states with  $L_{total} = 0$ . One of them is the state with one photon (no pairs), and the remaining 16 states correspond to matter excitations (no photons), that is, all possible combinations of one electron and one hole states with total angular momentum equal to zero.

As  $N_{pol}$  increases, the number of eigenstates of  $H$  rises, reaching around 18000 for  $N_{pol} = 10$ . We use Lanczos algorithms [10] to obtain the energies and wavefunctions of the lowest 20 states, which are used to write down the master equation for the density matrix. This number of states, 20, is chosen on the basis of two reasons. First, we want to keep the number of matrix elements,  $\rho_{FI}$ , between reasonable limits. And, second, in a sector with given  $N_{pol}$  we shall include all of the states,  $|I\rangle$ , with significant matrix elements,  $\langle F|a|I\rangle$ , between  $|I\rangle$  and the ground state in the sector with  $N_{pol} - 1$ . They are very important in the dynamics, as it will be shown below.

We draw in Fig. 1(a) the set of states used in this work for a detuning  $\Delta = -3$  meV. Notice the approximate linear dependence of the ground-state energy on  $N_{pol}$ , and the energy gap from the ground to the first excited state in each sector, roughly proportional to  $\sqrt{N_{pol}} g$ .

A sample of the matrix elements  $|\langle F|a|I\rangle|^2$  is represented in Fig. 1(b). Matrix elements are smeared out with a Lorentzian of width  $\Gamma = 0.1$  meV. The states  $|I\rangle$  correspond to  $N_{pol} = 2$ , whereas  $|F\rangle$  is the ground state in the  $N_{pol} = 1$  sector. The lower (LP) and upper polariton (UP) branches are clearly distinguished. Notice that the latter are included among the 20 states which participate in the dynamics. This is important because they substantially contribute to the population of the lowest state in each sector with given  $N_{pol}$ .

Now we come to the central point of the paper, the master equation for the density matrix and its stationary solution. The master equation is written as [11, 12]:

$$\begin{aligned} \frac{d\rho}{dt} = & -\frac{i}{\hbar} [H, \rho] + \frac{\kappa}{2} (2a\rho a^\dagger - a^\dagger a \rho - \rho a^\dagger a) \\ & + \frac{P}{2} \sum_{I,J} (2\sigma_{IJ}^\dagger \rho \sigma_{IJ} - \sigma_{IJ} \sigma_{IJ}^\dagger \rho - \rho \sigma_{IJ} \sigma_{IJ}^\dagger). \end{aligned} \quad (5)$$

The parameter  $\kappa$  accounts for photon losses through the cavity mirrors ( $\hbar\kappa \approx E_{gap}/Q$ , where  $Q$  is the cavity quality factor). In our calculations, we take  $\kappa = 0.1$  ps<sup>-1</sup>. Notice that  $\kappa \ll g$ , thus our model system works under the strong light-matter coupling regime. Other sources of losses such as, for example, spontaneous exciton decay are much less important and will not be considered. On the other hand, the parameter  $P$  is a pumping rate. In our modeling, incoherent pumping is supposed to come from highly excited excitonic states, which decay towards the lower polariton states through phonon emission. This is a kind of polariton reservoir. We will use a sort of homogeneous pumping, with equal probabilities for all states. To this end, we introduce lowering and rising operators,  $\sigma_{IJ}|I\rangle = |J\rangle$ ,  $\sigma_{IJ}^\dagger|J\rangle = |I\rangle$ . As we are employing a finite number of states (20) in each sector with given  $N_{pol} > 1$ , total pumping probabilities are finite. Notice that we are not including relaxation acting at the ‘‘horizontal’’ level in Fig. 1(a), i.e. causing the excited polariton states to decay towards the lowest states with the

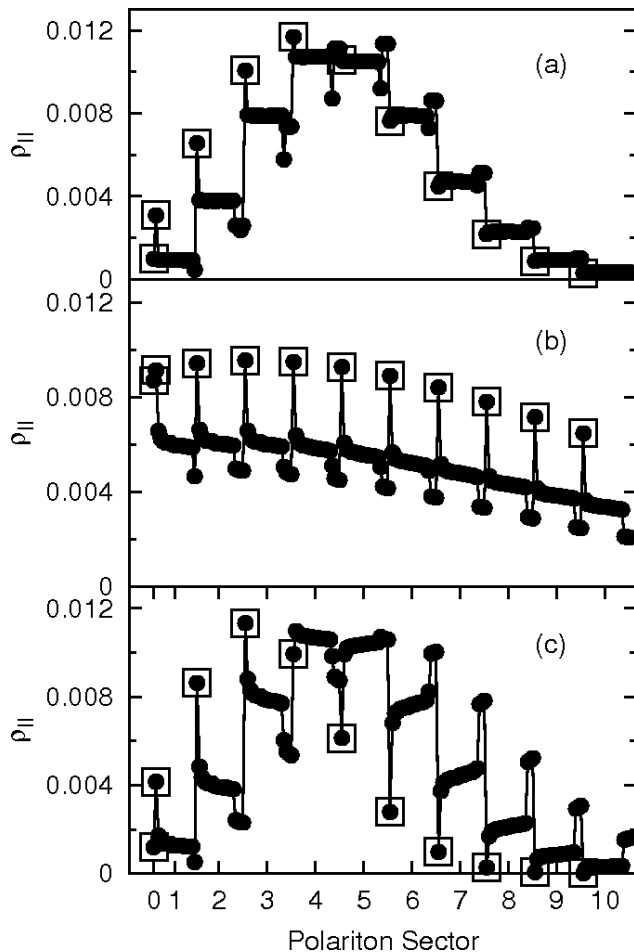


FIG. 2: (a) The occupations in each polariton sector. The detuning parameter is  $\Delta = -3$  meV, and the pumping rate is  $P = 0.01$  ps $^{-1}$ . Ground-state occupations are indicated by squares. (b) The best fit to the actual occupations with a grand canonical Gibbs distribution. (c) Best fit with a distorted grand canonical Gibbs distribution.

same  $N_{pol}$ . Thus, if the lowest polariton states become occupied in our simulation it is the result of dynamics and not of relaxation. The absence of phonon thermalization is also the reason why  $L_{total} = 0$  states are decoupled from other states with  $L_{total} \neq 0$ .

In the stationary limit, the r.h.s. of Eq. (5) is equal to zero. This set of homogeneous linear equations can be shown to be linearly dependent. Indeed, it can be easily verified that

$$\frac{d}{dt} \sum_I \rho_{II} = 0, \quad (6)$$

which corresponds to the conservation of probability,  $\sum_I \rho_{II} = 1$ . We replace the equation for  $\rho_{11}$  by the constraint  $\sum_I \rho_{II} = 1$  in order to obtain an inhomogeneous system:

$$\sum_{J,K} M_{FI,JK} \rho_{JK} = B_{FI}, \quad (7)$$

where  $M_{11,11} = 1$ , the rest of the matrix elements,  $M_{FI,JK}$ , are obtained from Eq. (5), and the components of the vector  $B_{FI}$  are zero, with the exception of  $B_{11} = 1$ . Only the occupations,  $\rho_{II}$ , and the ‘‘horizontal’’ coherences,  $\rho_{FI}$ , where  $F$  and  $I$  are states in the same  $N_{pol}$  sector, acquire nontrivial values as a result of solving Eq. (7). The other coherences are equal to zero.

We show in Fig. 2(a) the resulting occupations for  $\Delta = -3$  meV and  $P = 0.01$  ps $^{-1}$ . The mean number of polaritons is  $\langle N_{pol} \rangle = 4.77$ . In this case, the system is under the ‘‘polariton laser’’ regime [6]. That is, above threshold ( $\langle N_{pol} \rangle \sim 1$ ) and below saturation due to Fermi statistics ( $\langle N_{pol} \rangle$  much greater than 10 in the present model, which is called ‘‘photon laser’’ regime in Ref. 6).

The first point in the figure, enclosed by a square, corresponds to vacuum’s occupation. The next 17 points corresponds to states with  $N_{pol} = 1$ . Then, there are 20 states corresponding to  $N_{pol} = 2$ , etc. In order to facilitate lecture of the figure, we have indicated the first state in each sector by enclosing it with a square. We may notice that the ground-state occupations in sectors with  $N_{pol} < \langle N_{pol} \rangle$  are notably enhanced as compared with the rest of the states in the same sector. This is mainly the result of a transfer of population from ‘‘upper-polariton’’ states, following from the matrix elements illustrated in Fig. 1(b). Consequently, the ‘‘upper-polariton’’ occupations are depressed.

The computed horizontal coherences are three orders of magnitude smaller than the occupations. For  $\Delta = -3$  meV and  $P = 0.01$  ps $^{-1}$ , we obtained  $\sum_{I < J} |\rho_{IJ}| = 7.4 \times 10^{-4}$ , which should be compared with  $\sum_I \rho_{II} = 1$ . This means that the stationary  $\rho$  is approximately diagonal in the energy representation. This is the main result of the paper. We verified that the above statement holds for any values of the system’s parameters.

Once shown that  $H$  and  $\rho$  approximately commute, we can try to answer the question about whether the computed  $\rho$  can be obtained from a maximum entropy principle. In a first attempt, we fit the occupations to a grand canonical Gibbs distribution,  $\rho \sim \exp(-(E - \mu_1 N_{pol})/T_1)$ . For the situation represented in Fig. 2(a), we get the effective parameters,  $T_1 = 28.05$  meV, and  $\mu_1 = E_{gap} - 11.7$  meV. The r.m.s. deviation is 0.003, one fourth of the maximum values of  $\rho$ . Qualitatively, however, it gives a poor description of the actual occupations, as it can be seen in Fig. 2(b).

A second possibility for the fit is motivated by the results of paper [8], where the stationary  $\rho$  of a nonequilibrium system is obtained from the maximization of the entropy with an additional constraint in phase space. Then, we should find the extremum of the functional:

$P$ (ps $^{-1}$ )	$\mu_2 - E_{gap}$ (meV)	$T_2$ (meV)	$\alpha_2$ (meV $^{-2}$ )
0.001	-2.60	13.92	$1.4 \times 10^{-2}$
0.01	-0.51	8.37	$1.5 \times 10^{-3}$
0.1	-0.10	4.00	$6.9 \times 10^{-4}$

TABLE I: Effective parameters corresponding to the fit given by Eq. (10).  $\Delta = -3$  meV.

$$\begin{aligned}
\mathcal{S} = & -\sum_I \rho_{II} \ln(\rho_{II}) + a_1 \left( \sum_I \rho_{II} - 1 \right) \\
& + a_2 \left( \sum_I \rho_{II} E(I) - \langle E \rangle \right) + a_3 (Q(\rho) - \langle Q \rangle) \\
& + a_4 \left( \sum_I \rho_{II} N_{pol}(I) - \langle N_{pol} \rangle \right), \quad (8)
\end{aligned}$$

where  $a_1, \dots, a_4$  are Lagrange multipliers, and  $Q(\rho)$  is the constraint. It was argued in Ref. 8 that the requirements of additivity and commutativity with the Hamiltonian fix the form of the constraint,  $Q(\rho) = \sum_I \rho_{II}^q F(I)$ , where  $q$  is a kind of Tsallis index, and  $F$  commutes with  $\rho$ . We choose  $F = H - E_{gap} N_{pol}$ . The equation for  $\rho$ ,

$$\begin{aligned}
0 = & -\ln(\rho_{II}) - 1 + a_1 + a_2 E(I) + a_4 N_{pol}(I) \\
& + a_3 q \rho_{II}^{q-1} (E(I) - E_{gap} N_{pol}(I)), \quad (9)
\end{aligned}$$

under the assumption that the distortion is weak,  $q \sim 1$ , can be iteratively solved. Taking the first iteration, we get:

$$\rho \sim e^{-(E - \mu_2 N_{pol})/T_2 - \alpha_2 (E - E_{gap} N_{pol})(E - \mu_2 N_{pol})}. \quad (10)$$

The parameter  $\alpha_2 = a_3 q (q-1)$  is expected to be small. In our model, fitting the computed occupations to Eq. (10), we obtain  $T_2 = 8.42$  meV,  $\mu_2 = E_{gap} - 0.53$  meV, and  $\alpha_2 = 0.0015$  meV $^{-2}$ . The r.m.s. deviation is  $9 \times 10^{-4}$ , three times smaller than in the previous case. Qualitatively, the obtained distribution, represented in Fig. 2(c), is much more closer to the actual occupations. The analogs of lower and upper polariton states show the highest dispersion.

In Table I, we give the effective parameters for pumping powers in the interval from 0.001 to 0.1 ps $^{-1}$ . In these computations, we neglect coherences and extend Eqs. (7) for the occupations up to a maximum  $N_{pol} = 40$ . We notice that the dependence of the chemical potential on  $P$  is qualitatively the same as observed in experiments [13]. The effective temperature decreases with  $P$ , but for still higher values of the pumping starts increasing, as in the experiments. We stress, however, that the experimental fits cover a range in the emission angle, whereas our  $L = 0$  distribution is qualitatively related to  $k = 0$  states, responsible for the emission along the normal direction.

In conclusion, we have computed the stationary density matrix of a pumped polariton system, which comes from a dynamical master equation without thermalization mechanisms. The density matrix is shown to be approximately diagonal in the energy representation. Thus, a kind of quasiequilibrium is established. Although our model describes a quantum dot strongly interacting with the lowest photon mode of a thin microcavity, a quasiequilibrium of dynamical origin could also be present in the experiments described in Refs. [1, 2, 3]. We should notice in this respect that the similarity between lasing and a second-order phase transition was underlined long ago in the context of laser physics (see for example Ref. 12, Chapter 11, and references therein). The accumulated evidences on Bose-Einstein condensation of polaritons could be a present-day manifestation of this old idea.

A dynamical framework could be also the basis for the computation of the photoluminescence spectra, second-order coherence functions, etc in the present model [14]. Experimental facts such as the low threshold for polariton lasing, increase of linewidth with pumping power, etc are nicely (qualitatively) reproduced. In this context, our work for a multiexcitonic quantum dot [5, 7, 14] explores an intermediate (in the number of states) region between the single-level dot [11] and the infinite system (quantum well, see for example Refs. [15, 16]), where the system is simple enough to be studied by exact diagonalization methods, but complex enough to exhibit many of the properties of the infinite system.

We showed that the computed density matrix can be reasonably fitted to a weakly distorted grand canonical Gibbs distribution. The multi-polariton analogs of UP and LP branches are the states worst fitted. Let us stress that the same strategy of obtaining  $\rho$  from entropy maximization with an additional constraint in phase space can be applied [17], with success, to the description of experiments on metaequilibrium states in electron plasma columns [18].

This work was partially supported by the Programa Nacional de Ciencias Basicas (Cuba), the Universidad de Antioquia Fund for Research, and the Caribbean Network for Quantum Mechanics, Particles and Fields (ICTP).

- 
- [1] Hui Deng, D. Press, S. Gotzinger, et. al., Phys. Rev. Lett. 97 (2006) 146402.
  - [2] J. Kasprzak, M. Richard, S. Kundermann, et. al., Nature 443 (2006) 409.
  - [3] S. Christopoulos et. al., Phys. Rev. Lett. 98 (2007) 126405.
  - [4] F. Tassone, C. Piermarocchi, V. Savona, A. Quattropani, and P. Schwendimann, Phys. Rev. B 56 (1997) 7554; A.I. Tartakovskii, M. Emam-Ismael, R.M. Stevenson, et. al.,

- Phys. Rev. B 62 (2000) R2283; F. Tassone and Y. Yamamoto, Phys. Rev. B 59 (1999) 10830; T.D. Doan, H.T. Cao, D.B. Tran Thoai, and H. Haug, Phys. Rev. B 72 (2005) 085301.
- [5] H. Vinck-Posada, B.A. Rodriguez, P.S.S. Guimaraes, et. al., Phys. Rev. Lett. 98 (2007) 167405.
- [6] D. Bajoni, P. Senellart, E. Wertz, et. al., Phys. Rev. Lett. 100 (2008) 047401.
- [7] H. Vinck, B.A. Rodriguez and A. Gonzalez, Physica E 35 (2006) 99.
- [8] A. Cabo and S. Curilef, arXiv:0709.0069.
- [9] F. Baldovin and E. Orlandini, Phys. Rev. Lett. 96 (2006) 240602.
- [10] J.K. Cullum and R.A. Willoughby, Lanczos algorithms for large symmetric eigenvalue computations, Birkhauser, Boston, 1985.
- [11] F.P. Laussy, E. del Valle, and C. Tejedor, Phys. Rev. Lett. 101 (2008) 083601.
- [12] M.O. Scully and S. Subairy, Quantum Optics, Cambridge University Press, Cambridge, 2001.
- [13] H. Deng, G. Weihs, D. Snoke, et. al., PNAS 100 (2003) 15318.
- [14] C.A. Vera, H. Vinck-Posada, and A. Gonzalez, arXiv:0807.1137.
- [15] M.H. Szymanska, J. Keeling, and P.B. Littlewood, Phys. Rev. B 75 (2007) 195331.
- [16] P. Schwendimann and A. Quattropani, Phys. Rev. B 77 (2008) 085317.
- [17] A. Cabo, S. Curilef, N.G. Cabo-Bizet, C.A. Vera, and A. Gonzalez, to be submitted.
- [18] X.P. Huang and C.F. Driscoll, Phys. Rev. Lett. 72 (1994) 2187.